nature chemistry

Article

https://doi.org/10.1038/s41557-025-01960-3

Triplet state reactivity of iminium ions in organocatalytic asymmetric [2 + 2] photocycloadditions

Received: 2 December 2024

Accepted: 27 August 2025

Published online: 6 October 2025

Check for updates

Vasco Corti[1], Gianluca Simionato[1], Lorenzo Rizzo[1], Stefano A. Serapian[2], Giorgio Pelosi[3], Mirco Natali[4] & Luca Dell'Amico[1]

Organic transformations mediated by the transient formation of iminium ions have shown remarkable synthetic potential for the construction of enantioenriched molecules. The possibility to access their first singlet excited state (S_1) under light irradiation has led to the development of previously inaccessible transformations. However, the triplet state (T_1) reactivity remains limited and typically requires external photosensitizers. Here we show that structurally modified chiral iminium ions, integrated into extended π-systems, directly engage in T_1 reactivity. This modified conjugated architecture was designed to overcome the intrinsic photophysical limitations of conventional iminium ion chemistry, enabling access to previously inaccessible excited-state reaction manifolds. The resulting system allows organocatalytic enantioselective [2 + 2] photocycloadditions without the need for external sensitizers. Mechanistic studies, involving spectroscopic techniques and computational methods, elucidate the role of the T_1 intermediate as the key reactive intermediate.

The rationalization and understanding of reaction mechanisms in asymmetric organocatalysis have enabled its development and broad application in organic synthesis[1,2]. In the field of covalent organocatalysis, the traditional use of iminium-ion intermediates has established a powerful catalytic platform for the stereocontrolled construction of new chemical bonds, facilitating the nucleophilic conjugate addition at the β-carbon of unsaturated carbonyl compounds[3]. This activation mode led to the development of a plethora of catalytic asymmetric methods and to the synthesis of structurally diversified products. On the other hand, the pioneering studies of Mariano on the photochemistry of iminium ions revealed that the light-excited state reactivity of these species is sharply different from the one in the ground state. In fact, upon light excitation, iminium ions can behave as photo-oxidants, triggering the formation of radical species from suitable radical precursors or taking part in stereospecific photocycloadditions[4–7]. Recently, the combination of visible light with asymmetric organocatalysis allowed the discovery of previously uncharted chemical reactivities. These findings contributed to dissipate the general perception that highly energetic excited states are not suitable intermediates for stereoselective transformations[8]. In 2017, Melchiorre and co-workers showed that the excited state of catalytic chiral iminium ions can be efficiently used for the generation of radical species, which can be subsequently trapped in a stereoselective manner[8–11] (**I**; Fig. 1a). More recently, Alemán and co-workers developed an organocatalytic asymmetric [2 + 2] photocycloaddition in which the singlet excited state of iminium ions, transiently generated from acyclic conjugated ketones, is intercepted by various dienes to obtain optically active cyclobutane derivatives[12] (**II**; Fig. 1a). These advances have enabled access to previously untapped chemical space with well-defined three-dimensional architectures, which is central to the field of asymmetric synthesis. While the singlet excited state (S_1) reactivity of iminium ion has proved its generality for a variety of diverse transformations, the use of the

[1]Department of Chemical Sciences, University of Padova, Padua, Italy. [2]Department of Chemistry, University of Pavia, Pavia, Italy. [3]Department of Chemistry, Life Sciences and Environmental Sustainability, University of Parma, Parma, Italy. [4]Department of Chemical, Pharmaceutical and Agricultural Sciences, University of Ferrara, Ferrara, Italy. e-mail: luca.dellamico@unipd.it

https://doi.org/10.1038/s41557-025-01960-3

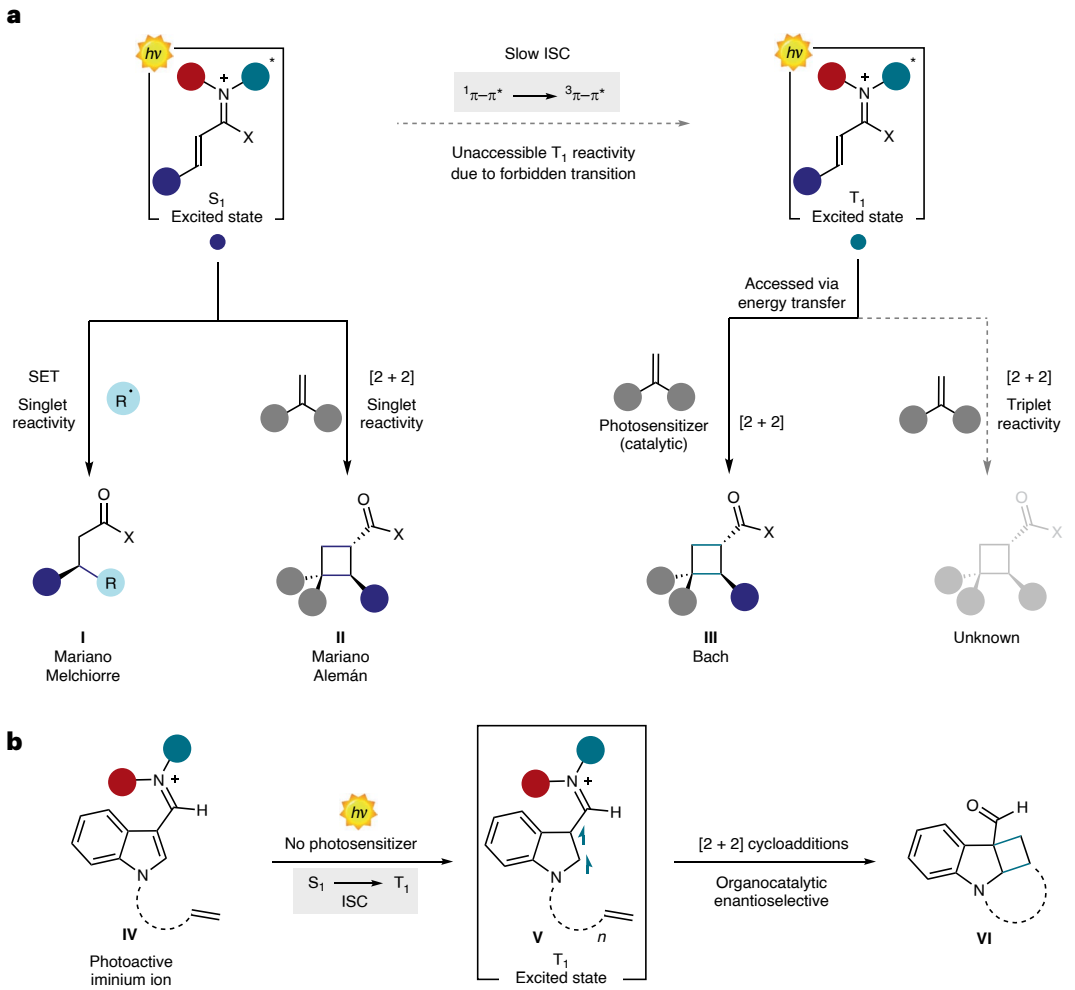

Fig. 1 | Photochemical reactivity of iminium ions. a, Reported types of reactivity in iminium ion-mediated catalysis. **b**, Leveraging the triplet excited state reactivity of iminium ions (**IV**) for the development of organocatalytic enantioselective [2 + 2] dearomative photocycloadditions. SET, single electron transfer. ISC, intersystem crossing.

triplet excited state (T_1) is far less developed. In a seminal work, Bach and co-workers reported that the T_1 state of iminium ions can be accessed by means of energy transfer catalysis, thanks to their lower triplet energy compared with the corresponding carbonyl compounds. The selection of an appropriate photosensitizer allowed the development of an asymmetric [2 + 2] photocycloaddition of the chiral iminium ions and various alkenes via energy transfer catalysis[13,14] (**III**; Fig. 1a).

Leveraging the T_1 reactivity of chiral iminium ions under direct excitation remains an unmet goal for the synthetic chemical community. In fact, the direct excitation of transiently generated chiral iminium ions to reach their T_1 state via intersystem crossing (ISC) would provide an attractive synthetic strategy for the development of innovative asymmetric photocycloadditions[15–20] to obtain enantioenriched cyclic derivatives[21] without the use of an external photocatalyst. However, this approach is hampered by the intrinsic photophysical properties of iminium ions. While conjugated carbonyl compounds can efficiently undergo ISC from their S_1 state to the corresponding T_1 state (^1n–π^* to $^3\pi$–π^*) engaging in [2 + 2] photocycloadditions, the photochemistry of the analogous iminium ions is governed by their singlet reactivity, as the ISC involves the forbidden transition $^1\pi$–π^* to $^3\pi$–π^* (refs. 6,7,13,14,22).

Despite these conceptual rules on the reactivity of classical conjugated iminium ions, we questioned whether altering the chemical nature of the conjugated system, such as its incorporation into heteroaromatics, could be the key strategy to access their elusive T_1 reactivity. For example, the indole moiety has been already used to develop [2 + 2] dearomative photocycloadditions[23–26], mostly via energy transfer catalysis[27–34]. We thus identified indole-3-carboxaldehyde as a promising candidate for our investigations. Embedding the conjugated iminium ion within a π-extended aromatic framework could mitigate the inherent photophysical limitations that typically hinder their T_1 reactivity. This approach, in turn, could enable catalytic enantioselective [2 + 2] dearomative photocycloadditions—a reaction class that remains markedly underexplored[35,36]. In fact, while the cyclobutane core is present in a variety of bioactive drugs and natural products, including paesslerin A[37], rumphellaone A[38] or the Food and Drug Administration-approved drug apaludamide[39], its enantioselective construction still represents an open challenge for the scientific community.

Herein, we describe the successful realization of an organocatalytic asymmetric [2 + 2] photocycloaddition involving the key reactivity of the T_1 state of photoactive iminium ions (Fig. 1b). This methodology relies on the formation of intermediate **IV** and its ability to access, upon light absorption and ISC, a reactive T_1 state **V** that undergoes a stereoselective dearomative [2 + 2] photocycloaddition, providing a wide variety of enantioenriched polycyclic products **VI**. We demonstrated that specific primary-amine organocatalysts, classically used under polar reactivity, can efficiently catalyse stereoselective transformations involving highly energetic excited intermediates. Photophysical studies and transient spectroscopy revealed the nature of the reactive excited state. Time-dependent density functional theory (TD-DFT) and density functional theory (DFT) study calculations were conducted to shed light on the formation and nature of this fleeting intermediate.

https://doi.org/10.1038/s41557-025-01960-3

Results

Optimization studies

At the outset of our studies, we decided to test the enantioselective intramolecular [2 + 2] photocycloaddition of 1-(pent-4-enoyl)-1*H*-indole-3-carbaldehyde (**1**) in the presence of trifluoroacetic acid (TFA) and the Jørgensen–Hayashi organocatalyst **2a** (20 mol%) under light irradiation using a Kessil lamp (427 nm). No product formation was observed after 24 h (Table 1, entry 1). We assumed that the high degree of steric hindrance of the organocatalyst, combined with the poor electrophilic character of aldehyde **1**, renders the condensation process inefficient. On the other hand, the use of primary amine-based organocatalysts immediately delivered more satisfactory results (Table 1, entries 2–4). Chiral diamine **2d** provided the desired product **3** in 62% yield and 91% enantiomeric excess (e.e.). A solvent screening identified $CHCl_3$ as the optimal for this transformation (Supplementary Table 2). Carrying out the reaction in the presence of an excess of acid additive improved the reaction yield up to 97% while shortening the reaction time from 24 h to 6 h (Table 1, entry 5; Supplementary Table 3). Finally, we performed a series of control experiments to verify the photochemical and radical nature of the transformation (Table 1, entries 6–8). The reaction does not occur in the absence of light nor of the organocatalyst, and the product formation is partially suppressed when performing the reaction under air.

Mechanistic investigations

We next turned our attention to the investigation of the reaction mechanism. Initially, we verified the capability of iminium ion **4** to absorb visible light. Indeed, upon mixing an equimolar amount of aldehyde **1** and organocatalyst **2d** in the presence of TFA, a new absorption band appears in the visible region of the spectrum, thus suggesting the formation of the photoactive intermediate **4** (ref. 10; Fig. 2a). We then investigated one of the most intriguing aspects of this transformation, namely, the nature of the excited state of the iminium ion **4** that is involved in the enantioselective [2 + 2] cycloaddition. To this end, we prepared iminium ion **5** that lacks the terminal olefin functional group. While this species cannot react in the photocycloaddition process, it was used as a model compound to compare its photophysical behaviour with the reactive intermediate **4**. We first performed steady-state luminescence measurements upon excitation at 360 nm to follow the fate of the singlet excited state in **4** and **5**. Both compounds display an intense emission centred at 445 nm, which can be assigned to fluorescence from the S_1 state of the iminium ion. Importantly, the fluorescence quantum yield (Φ) is comparable for both **4** and **5**, as is the fluorescence lifetime measured by time-correlated single-photon counting (TCSPC; Fig. 2a; for further details, see Supplementary Figs. 4–7 and the related discussion). These results strongly suggest that the S_1 state cannot be responsible for the observed reactivity. We then performed laser flash photolysis (LFP) studies on both **4** and **5** to monitor their T_1 state. For both compounds, a similar transient absorption spectrum is detected upon laser excitation at 355 nm, which is characterized by ground state bleaching below 400 nm, a sharp absorption centred at 410 nm and a broad absorption in the red portion of the visible spectrum (Fig. 2b,c). Accordingly, the transient species can be mainly assigned to the T_1 state of the iminium ion. In the case of the unreactive iminium **5**, the transient absorption signal at 700 nm decays towards the baseline within a hundred microseconds (Fig. 2d). The decay kinetics of compound **5** is sensitive to the presence of dioxygen, and a lifetime of $\tau = 12$ µs can be estimated under N_2-purged conditions. Both of these observations support that the transient species detected by LFP is the triplet excited state of the iminium ion. More importantly, in the case of the iminium **4**, the transient signal at 700 nm decays more rapidly (Fig. 2d), indicating quenching of the triplet state in the presence of the olefin functional group. Thus, this experimental evidence strongly corroborates the participation of the T_1 state in the [2 + 2] reaction leading to the formation of the desired cycloadduct.

To further prove the triplet reactivity in the present reaction, a control experiment under the optimized reaction conditions was performed in the presence of 1 equivalent of the triplet quencher 2,5-dimethylhexa-2,4-diene. As shown in Fig. 2e, no product formation was observed, with almost quantitative recovery of the starting material **1**. On the other hand, carrying out the reaction in the presence of an iridium-based triplet sensitizer greatly accelerated the reaction rate, albeit in lower enanantioselectivity due to the poor discrimination between the activation of substrate **1** and intermediate **4** (for additional results and discussion, see Supplementary Scheme 1).

Finally, substrates **7**-(*E*) and **7**-(*Z*) were employed as structural probes to further confirm our mechanistic proposal[6] (Fig. 2f). Indeed, [2 + 2] photocycloadditions that occur at the S_1 state are typically stereospecific processes due to the concerted character of their mechanism, and for this reason, the geometry of the double bond is retained into the corresponding product. On the other hand, stereoconvergent [2 + 2] photocycloadditions are indicative of a step-wise mechanism, which typically involves T_1 reactivity. For this reason, a series of experiments using either **7**-(*E*) or **7**-(*Z*) were performed under the optimized reaction conditions. While substrate **7**-(*E*) furnished the corresponding cycloadduct in 6.5:1 diastereoisomeric ratio (d.r.) and 50% yield after 2 h, a lower d.r. (1.5:1 in the same major diastereoisomer) was obtained when employing **7**-(*Z*). The formation of both diastereoisomers, regardless of the double bond geometry, suggests that the present photocycloaddition occurs through a step-wise mechanism that involves the T_1 state of the iminium ion intermediate. Furthermore, the diastereoisomeric ratio is constant even at lower conversion values, ruling out a scenario in which one isomer of the product interconverts into the other during the reaction course[6].

Table 1 | Selected results from the reaction optimisation

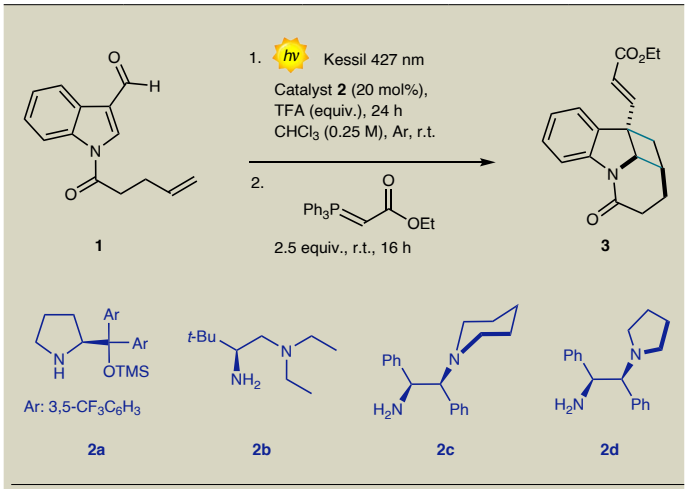

Entry[a]	Catalyst 2	TFA (equiv.)	Yield (%)[b]	e.e. (%)[c]
1[d]	**2a**	1	<5	n.d.
2[d]	**2b**	1	64	63
3[d]	**2c**	1	67	89
4[d]	**2d**	1	62	91
5	**2d**	2.5	97	92
6	No catalyst	2.5	<5	n.d.
7	**2d**, no light	2.5	<5	n.d.
8	**2d**, air	2.5	44	n.d.

n.d., not determined [a]Substrate **1** (0.1 mmol), organocatalyst (20 mol%, 0.02 mmol), TFA (equiv.), $CHCl_3$ (0.4 ml) and inert atmosphere. [b]Reaction yields were measured by ^{1}H NMR analysis of the crude reaction mixture using dibromomethane as the internal standard. [c]The e.e. values were determined by chiral stationary phase ultra-performance convergence chromatography (UPC^2) after derivatization of the [2+2] cycloadduct with (carbethoxymethylene) triphenylphosphorane. [d]1,2-Dichloroethane was used in place of $CHCl_3$.

https://doi.org/10.1038/s41557-025-01960-3

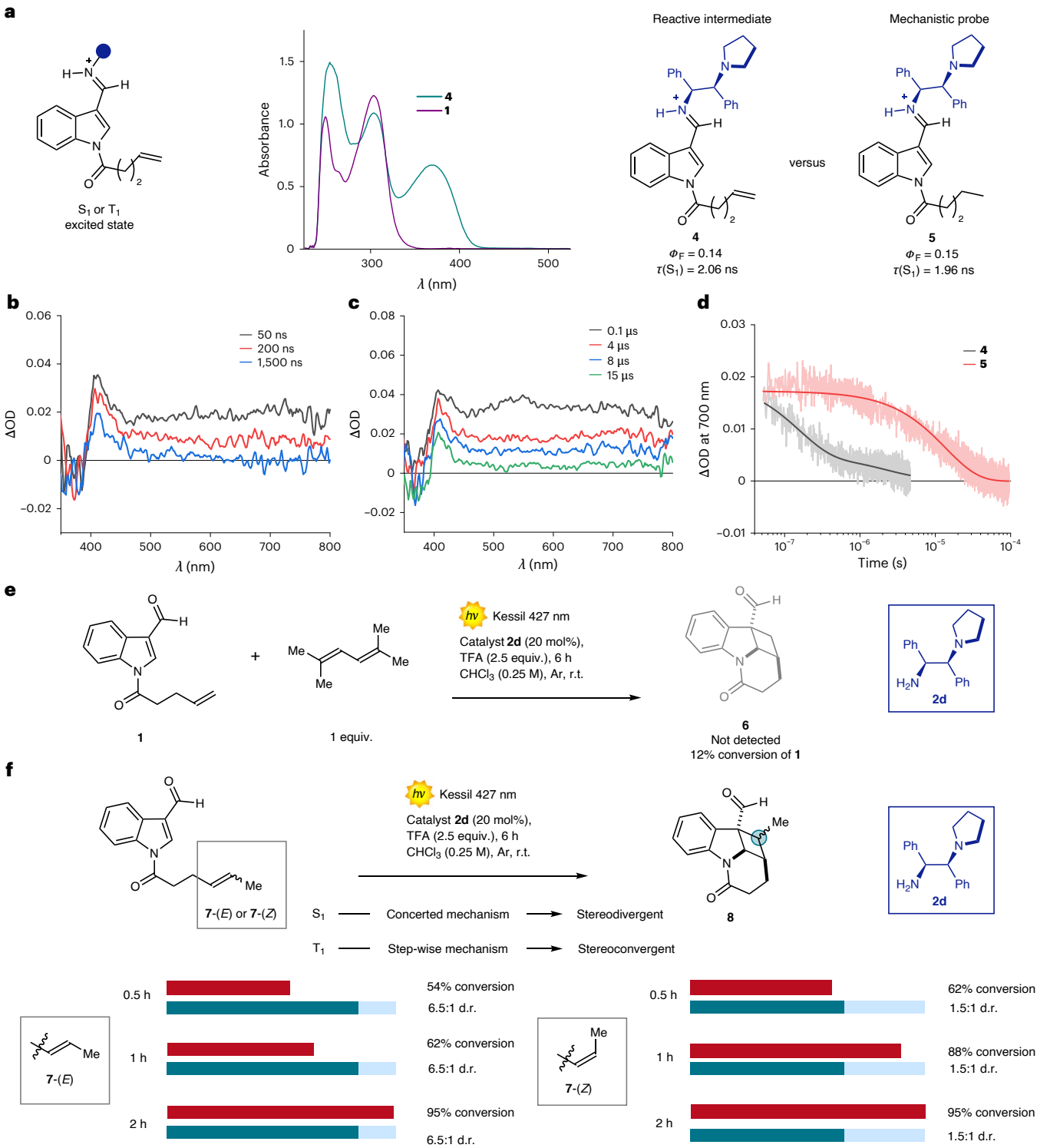

Fig. 2 | Mechanistic investigations. a, Steady-state luminescence studies. UV–vis absorption spectroscopy to verify the formation of iminium ion **4** by formation of a new band in the visible region. Comparison of the fluorescence quantum yields Φ_F and fluorescence lifetimes $\tau(S_1)$ of compounds **4** and **5**. λ is the wavelength of electromagnetic radiation. **b**, Transient absorption spectra of **4**. **c**, Transient absorption spectra of **5**. **d**, Kinetic decay measured at 700 nm of the triplet excited state of **4** compared with **5**. OD, optical density. **e**, Control experiment using a triplet quencher. r.t., room temperature. **f**, Stereochemical outcome of the organocatalytic enantioselective [2 + 2] photocycloaddition starting from the two diastereoisomers **7**-(*E*) and **7**-(*Z*). Depending on the stereochemical outcome (stereodivergent versus stereoconvergent process), the involvement of a singlet or triplet excited state can be suggested. The epimerization of the additional stereogenic centre is ruled out by the unchanged d.r. value during the reaction course.

Computational investigations

To support the proposed reaction manifold and gain information on the nature of the involved intermediates and transitions, we carried out a series of DFT and TD-DFT studies[40] (Fig. 3). All calculations are provided electronically in the ioChem-BD repository[41].The calculations show that photoexcitation of **4** (S_0) leads to the relaxed S_1 state intermediate **4** (S_1)

https://doi.org/10.1038/s41557-025-01960-3

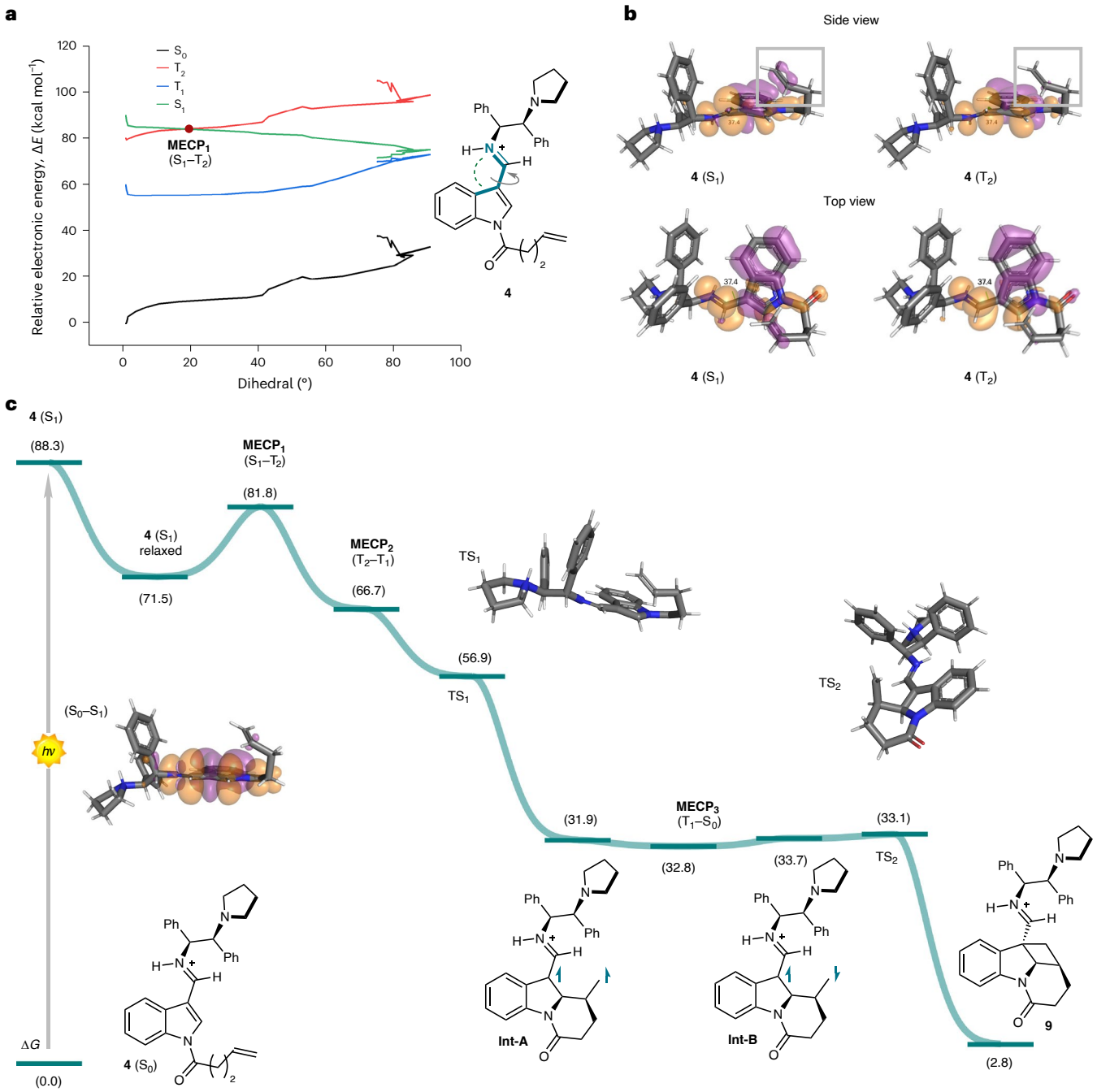

Fig. 3 | TD-DFT and DFT investigations. a, Relative electronic energy profile for the unconstrained TD-DFT minimization (relaxation) of **4** (S_1) after photoexcitation of **4** (S_0), viewed with out-of-plane iminium distortion towards the *Re* face of the C=C indole bond involved in the [2 + 2] cycloaddition. The reaction coordinate is the CCCN dihedral marked in green in **4** (0° when fully planar): surfaces for S_0, T_1 and T_2 are also shown for comparison; all other low-lying excited states are omitted for clarity. **b**, Representations of the S_1 and the T_2 states at $MECP_1$ (S_1–T_2) as electron–hole pairs (difference between squared natural transition orbitals (NTOs); orange areas denote maximum localization of the excited electron). **c**, The relative free energy profile (ΔG) of the proposed reaction pathway for the organocatalytic enantioselective [2 + 2] photocycloaddition. Only the pathway leading to the observed enantiomer is presented.

in which the iminium moiety is no longer planar owing to a distortion out of the plane of the indole core towards the *Re* face of its reactive C=C (+75.2°, for further details see 'Computational studies' section of Supplementary Information and Supplementary Fig. 16). The relaxed **4** (S_1) intermediate is not productive for the observed reactivity (see the discussion related to Supplementary Fig. 17), confirming that the reaction must proceed through a triplet state. Monitoring the potential energy surfaces of the other excited states of iminium ion **4** (S_1) as the iminium distorts towards the *Re* face of the indole C = C, we observed that the S_1 surface comes to within 1.66 kcal mol^{-1} of the T_1 surface but never crosses it (Fig. 3a and Supplementary Fig. 18).

Interestingly, it was possible to locate a minimum energy crossing point (**$MECP_1$**) between the S_1 and the T_2 excited states (for example, at +37.4° in the case under examination in Fig. 3b). We concluded from these findings that the observed triplet reactivity should prevalently transit through the T_2 state, with direct $S_1 \rightarrow T_1$ ISC remaining unlikely. While a fraction of the photoexcited **4** (S_1) could directly cross to T_2 through **$MECP_1$**, since the S_1–T_2 transition is spin-prohibited, it is likely

https://doi.org/10.1038/s41557-025-01960-3

Table 2 | Generality of the organocatalytic enantioselective [2+2] cycloaddition for the dearomatization of the indole core

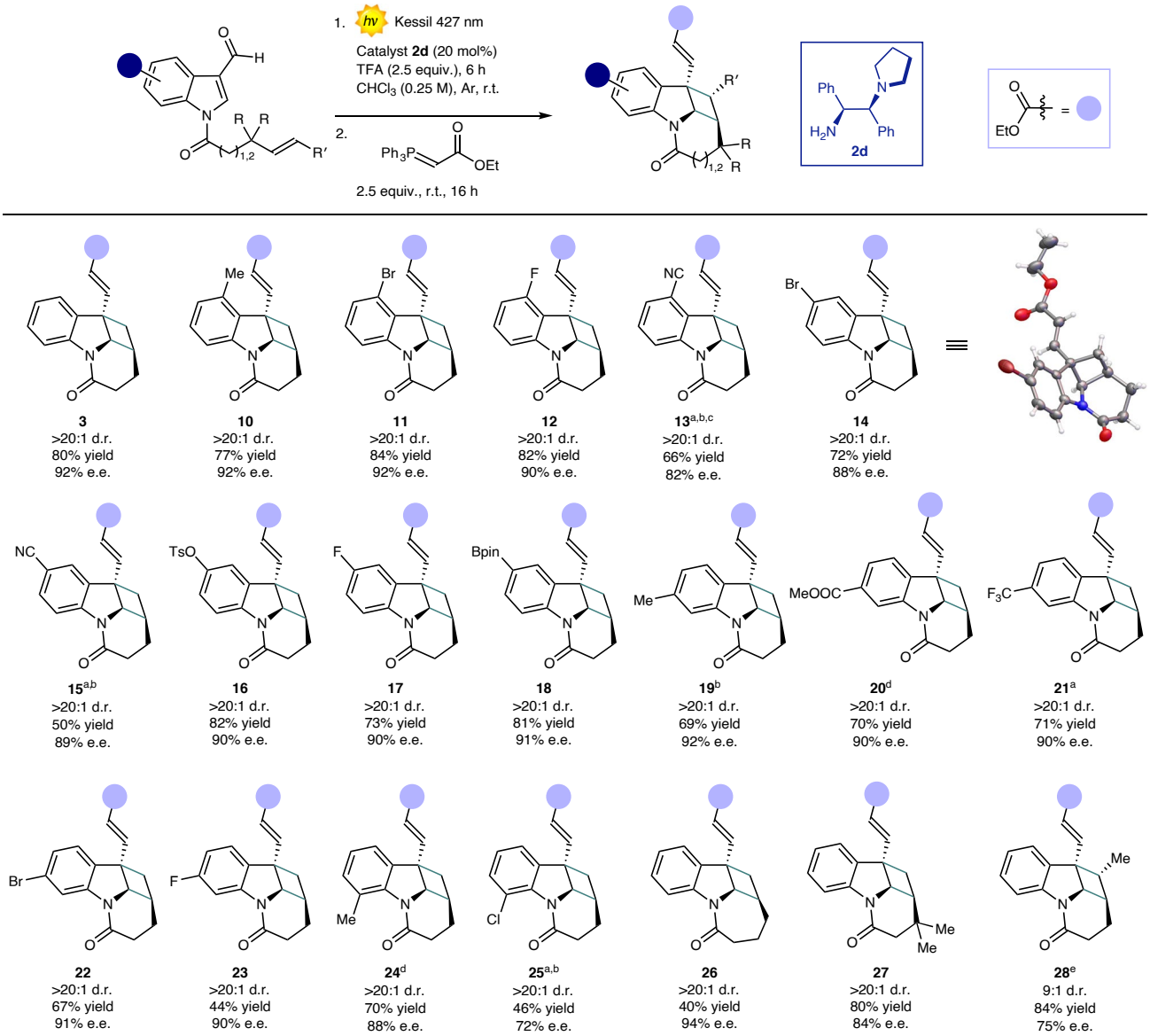

[a]Kessil lamp at 400 nm. [b]Reaction time of 18 h. [c]Solvent mixture: $CHCl_3$/PhCl (1:1). [d]Reaction time of 12 h. [e]Reaction time of 3 h and 0 °C.

that the majority of photoexcited molecules reach the relaxed photoexcited intermediate **4** (S_1) before climbing back up to the **MECP$_1$** (Fig. 3b). Here, a precise quantification of spin–orbit coupling effects governing the S_1–T_2 transition is not performed as it requires higher level calculations.

Subsequent relaxation from **MECP$_1$** on the T_2 surface shows that, as the iminium moiety is further on its way back to planarity from +37.4°, the T_1 state is readily encountered at a second **MECP$_2$**. This new T_1 state further relaxes to a first order transition state TS_1 that preludes the formation of the first C–C bond. The resulting intermediate (**Int-A**) can then cross from the T_1 state to the open shell singlet (**Int-B**) with a virtually barrierless transition. Finally, the transition state TS_2 leads to radical–radical recombination of **Int-B**, providing the final cycloadduct **9**. A complete mechanistic description of the reaction, including investigation of possible sources of enantioselectivity, is provided in the 'Computational studies' section of Supplementary Information, along with orbital representations of salient stationary points along the favoured pathway.

Scope of the reaction

While 4CzIPN (2,4,5,6-tetrakis(9*H*-carbazol-9-yl) isophthalonitrile) was used for the preparation of racemic samples, the generality of the reaction was evaluated using the optimized reaction conditions. A wide variety of functional groups could be substituted at the indole core without substantially affecting the reaction yield or stereoselectivity (Table 2; products **10**–**25**, 44–84% yield and 72–92% e.e.).

X-ray analysis on a single crystal of product **14** was used to infer both the absolute and relative configuration of the [2 + 2] cycloadduct, and the configuration of all the other products was assigned by analogy. It was also possible to introduce variations at the tethered olefin, furnishing products **26** and **27** with comparable values of yield and enantioselectivity (40% and 80% yield and 84% and 94% e.e., respectively).

Finally, the cyclobutane derivative **28** featuring four contiguous stereogenic centres was obtained in 84% yield, 75% e.e. and 9:1 d.r. We next focussed our efforts on expanding the generality of our approach to an intermolecular version of the reaction. Remarkably, indole **29** reacted smoothly with a series of different alkenes delivering

https://doi.org/10.1038/s41557-025-01960-3

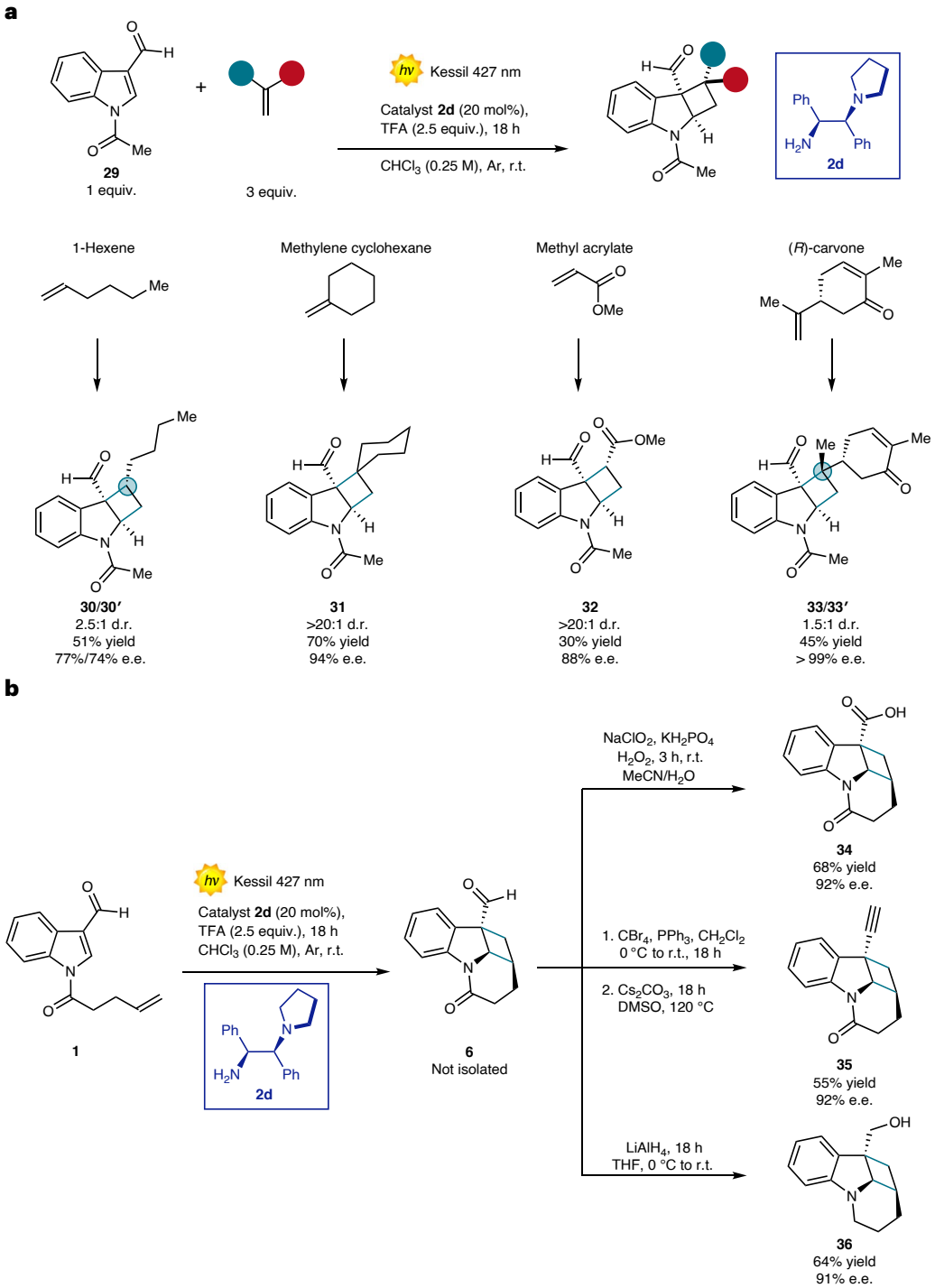

Fig. 4 | Expanding the generality of the developed catalytic approach. **a**, Intermolecular enantioselective [2 + 2] cycloadditions with external olefins. **b**, Synthetic elaborations of the optically active cycloadduct. From top to bottom: Pinnick oxidation, Corey–Fuchs homologation and concomitant reduction of amide and aldehyde functionalities. Upon acid wash to remove the organocatalyst, the crude product of the photochemical reaction was used directly in the subsequent transformation without any further purification. The yield of the synthetic elaborations was measured on the basis of ^{1}H NMR analysis to determine the amount of cycloadduct **6** used as the starting material.

the desired enantioenriched cyclobutanes with satisfactory levels of yield under the very same reaction conditions (Fig. 4a). For example, products **30** and **30′** were isolated using 1-hexene as a reaction partner, providing 51% combined yield, 2.5:1 d.r. and good levels of enantioselectivity (74–77%). Methylene cyclohexane gave excellent results, furnishing the [2 + 2] cycloaddition product **31** in 70% yield and 94% e.e. as a single diastereoisomer. On the other hand, carrying out the reaction in presence of electron-poor olefins such as methyl acrylate provided the corresponding cycloadduct in a lower yield of 30%, with very high stereocontrol (88% e.e.) as a single diastereoisomer (**32**; Fig. 4a). We next performed the reaction with the natural compound (*R*)-(−)-carvone. Interestingly, the corresponding product formed in 45% yield as a 1.5:1 mixture of diastereoisomers. Both cycloadducts could be isolated, providing access to complex structures featuring four contiguous stereogenic centres along with two contiguous all-carbon quaternary stereogenic centres (**33** and **33′**; Fig. 4a). Finally, we carried out a series

of synthetic manipulations on the optically active cycloadduct **6** to demonstrate that the polycyclic scaffold can be further manipulated (Fig. 4b). It was possible to transform the aldehyde moiety either into a carboxylic acid (product **34** in 68% yield and 92% e.e.) or a terminal alkyne (**35** in 55% yield and 92% e.e.): two privileged functionalities for bioconjugation processes. Alternatively, the concomitant reduction of the amide and the aldehyde group rendered product **36** in 64% yield and 91% e.e.

Conclusions

We have shown that structural modifications of iminium ions can lead to previously inaccessible reactivities. Their T_1 state enabled an organocatalytic enantioselective [2 + 2] photocycloaddition, which proceeds in the absence of any external photocatalyst. Using UV–vis and transient spectroscopy, we established that the triplet state of the iminium ion is the key reactive intermediate in this transformation. The proposed reaction pathway was further supported by DFT calculations, which revealed a singlet–triplet intersystem crossing ($S_1 \rightarrow T_2$) facilitating access to the reactive T_1 state. The generality of the process was demonstrated across a range of substrates bearing diverse functional groups, affording the desired products in consistently high yields and with excellent enantioselectivities. Moreover, the catalytic system was successfully extended to the intermolecular variant of the reaction, including complex alkene partners such as (*R*)-(−)-carvone. These findings establish an alternative platform in the field of catalytic asymmetric dearomatization reactions harnessing excited-state reactivity.

Online content

Any methods, additional references, Nature Portfolio reporting summaries, source data, extended data, supplementary information, acknowledgements, peer review information; details of author contributions and competing interests; and statements of data and code availability are available at https://doi.org/10.1038/s41557-025-01960-3.

References

1. Dalko, P. I. (ed.) *Comprehensive Enantioselective Organocatalysis: Catalysts, Reactions, and Applications* (Wiley-VCH, 2013).
2. MacMillan, D. W. C. The advent and development of organocatalysis. *Nature* **455**, 304–308 (2008).
3. Erkkilä, A., Majander, I. & Pihko, P. M. Iminium catalysis. *Chem. Rev.* **107**, 5416–5470 (2007).
4. Mariano, P. S. The photochemistry of iminium salts and related heteroaromatic systems. *Tetrahedron* **39**, 3845–3879 (1983).
5. Mariano, P. S. Electron-transfer mechanisms in photochemical transformations of iminium salts. *Acc. Chem. Res.* **16**, 130–137 (1983).
6. Cai, X., Chang, V., Chen, C., Kim, H.-J. & Mariano, P. S. A potentially general method to control relative stereochemistry in enone–olefin 2+2-photocycloaddition reactions by using eniminium salt surrogates. *Tetrahedron Lett.* **41**, 9445–9449 (2000).
7. Chen, C., Chang, V., Cai, X., Duesler, E. & Mariano, P. S. A general strategy for absolute stereochemical control in enone-olefin [2 + 2] photocycloaddition reactions. *J. Am. Chem. Soc.* **123**, 6433–6434 (2001).
8. Silvi, M. & Melchiorre, P. Enhancing the potential of enantioselective organocatalysis with light. *Nature* **554**, 41–49 (2018).
9. Arceo, E., Jurberg, I., Álvarez-Fernández, A. & Melchiorre, P. Photochemical activity of a key donor–acceptor complex can drive stereoselective catalytic α-alkylation of aldehydes. *Nat. Chem* **5**, 750–756 (2013).
10. Silvi, M., Verrier, C., Rey, Y., Buzzetti, L. & Melchiorre, P. Visible-light excitation of iminium ions enables the enantioselective catalytic β-alkylation of enals. *Nat. Chem.* **9**, 868–873 (2017).
11. Zou, Y.-Q., Hörmann, F. M. & Bach, T. Iminium and enamine catalysis in enantioselective photochemical reactions. *Chem. Soc. Rev.* **47**, 278–290 (2018).
12. Rigotti, T., Mas-Ballesté, R. & Alemán, J. Enantioselective aminocatalytic [2 + 2] cycloaddition through visible light excitation. *ACS Catal.* **10**, 5335–5346 (2020).
13. Hörmann, F. M., Chung, T. S., Rodriguez, E., Jakob, M. & Bach, T. Evidence for triplet sensitization in the visible-light-induced [2+2] photocycloaddition of eniminium ions. *Angew. Chem. Int. Ed.* **57**, 827–831 (2018).
14. Hörmann, F. M. et al. Triplet energy transfer from ruthenium complexes to chiral eniminium ions: enantioselective synthesis of cyclobutanecarbaldehydes by [2+2] photocycloaddition. *Angew. Chem. Int. Ed.* **59**, 9659–9668 (2020).
15. Brimioulle, R. & Bach, T. Enantioselective Lewis acid catalysis of intramolecular enone [2+2] photocycloaddition reactions. *Science* **342**, 840–843 (2013).
16. Du, J., Skubi, K. L., Schultz, D. M. & Yoon, T. P. A dual-catalysis approach to enantioselective [2 + 2] photocycloadditions using visible light. *Science* **344**, 392–396 (2014).
17. Blum, T. R., Miller, Z. D., Bates, D. M., Guzei, I. A. & Yoon, T. P. Enantioselective photochemistry through Lewis acid–catalyzed triplet energy transfer. *Science* **354**, 1391–1395 (2016).
18. Yoon, T. P. Photochemical stereocontrol using tandem photoredox–chiral Lewis acid catalysis. *Acc. Chem. Res.* **49**, 2307–2315 (2016).
19. Poplata, S., Tröster, A., Zou, Y.-Q. & Bach, T. Recent advances in the synthesis of cyclobutanes by olefin [2+2] photocycloaddition reactions. *Chem. Rev.* **116**, 9748–9815 (2016).
20. Genzink, M. J., Kidd, J. B., Swords, W. B. & Yoon, T. P. Chiral photocatalyst structures in asymmetric photochemical synthesis. *Chem. Rev.* **122**, 1654–1716 (2022).
21. Cox, B., Booker-Milburn, K. I., Elliott, L. D., Robertson-Ralph, M. & Zdorichenko, V. Escaping from flatland: [2 + 2] photocycloaddition; conformationally constrained sp^3-rich scaffolds for lead generation. *ACS Med. Chem. Lett.* **10**, 1512–1517 (2019).
22. El-Sayed, M. A. Triplet state. Its radiative and nonradiative properties. *Acc. Chem. Res.* **1**, 8–16 (1968).
23. James, M. J., Schwarz, J. L., Strieth-Kalthoff, F., Wibbeling, B. & Glorius, F. Dearomative cascade photocatalysis: divergent synthesis through catalyst selective energy transfer. *J. Am. Chem. Soc.* **140**, 8624–8628 (2018).
24. Hu, N. et al. Catalytic asymmetric dearomatization by visible-light-activated [2+2] photocycloaddition. *Angew. Chem. Int. Ed.* **57**, 6242–6246 (2018).
25. Stegbauer, S., Jandl, C. & Bach, T. Enantioselective Lewis acid catalyzed *ortho* photocycloaddition of olefins to phenanthrene-9-carboxaldehydes. *Angew. Chem. Int. Ed.* **57**, 14593–14596 (2018).
26. Ma, J. et al. Photochemical intermolecular dearomative cycloaddition of bicyclic azaarenes with alkenes. *Science* **371**, 1338–1345 (2021).
27. Großkopf, J., Kratz, T., Rigotti, T. & Bach, T. Enantioselective photochemical reactions enabled by triplet energy transfer. *Chem. Rev.* **122**, 1626–1653 (2022).
28. Strieth-Kalthoff, F., James, M. J., Teders, M., Pitzera, L. & Glorius, F. Energy transfer catalysis mediated by visible light: principles, applications, directions. *Chem. Soc. Rev.* **47**, 7190–7202 (2018).
29. Zhu, M., Zheng, C., Zhang, X. & You, S.-L. Synthesis of cyclobutane-fused angular tetracyclic spiroindolines via visible-light-promoted intramolecular dearomatization of indole derivatives. *J. Am. Chem. Soc.* **141**, 2636–2644 (2019).
30. Oderinde, M. S. et al. Synthesis of cyclobutane-fused tetracyclic scaffolds via visible-light photocatalysis for building molecular complexity. *J. Am. Chem. Soc.* **142**, 3094–3103 (2020).

31. Zhang, Z. et al. Photocatalytic intramolecular [2 + 2] cycloaddition of indole derivatives via energy transfer: a method for late-stage skeletal transformation. *ACS Catal.* **10**, 10149–10156 (2020).
32. Oderinde, M. S. et al. Photocatalytic dearomative intermolecular [2 + 2] cycloaddition of heterocycles for building molecular complexity. *J. Org. Chem.* **86**, 1730–1747 (2021).
33. Zhu, M., Zhang, X., Zheng, C. & You, S.-L. Energy-transfer-enabled dearomative cycloaddition reactions of indoles/pyrroles via excited-state aromatics. *Acc. Chem. Res.* **55**, 2510–2525 (2022).
34. Oderinde, M. S. et al. Advances in the synthesis of three-dimensional molecular architectures by dearomatizing photocycloadditions. *Tetrahedron* **103**, 132087 (2022).
35. Sun, N. et al. Enantioselective [2+2]-cycloadditions with triplet photoenzymes. *Nature* **611**, 715–720 (2022).
36. Wang, J. et al. Enantioselective [2 + 2] photocycloreversion enables de novo deracemization synthesis of cyclobutanes. *J. Am. Chem. Soc.* **146**, 22840–22849 (2024).
37. Inanaga, K., Takasu, K. & Ihara, M. Rapid assembly of polycyclic substances by a multicomponent cascade (4 + 2)–(2 + 2) cycloadditions: total synthesis of the proposed structure of paesslerin A. *J. Am. Chem. Soc.* **126**, 1352–1353 (2004).
38. Chung, H. M., Chen, Y. H., Lin, M. R., Su, J. H. & Wang, W. H. Rumphellaone A, a novel caryophyllane-related derivative from the gorgonian coral *Rumphella antipathies*. *Tetrahedron Lett.* **51**, 6025–6027 (2010).
39. Shen, J. et al. Apalutamide efficacy, safety and wellbeing in older patients with advanced prostate cancer from phase 3 randomised clinical studies TITAN and SPARTAN. *Br. J. Cancer* **130**, 73–81 (2024).
40. Álvarez-Moreno, M. et al. Managing the computational chemistry big data problem: the ioChem-BD platform. *J. Chem. Inf. Model.* **55**, 95–103 (2015).
41. Serapian, S. A. Iminium-ion-2+2-photocycloaddition. *ioChem-BD* https://doi.org/10.19061/iochem-bd-6-426 (2025).

Methods

General procedure for the intramolecular preparation of enantioenriched cycloadducts

A 4-ml screw-cap vial equipped with a magnetic stirring bar was charged with the indole substrate (1 equiv.) and organocatalyst **2d** (20 mol%) and filled with argon. Then, $CHCl_3$ (0.25 M) was added after being dried with 4-Å molecular sieves and degassed by sparging argon for 10 min. TFA was added (2.5 equiv.), and the vial was sealed. The mixture was irradiated until full consumption of the starting material with a Kessil lamp set at 50% of its maximum output power, unless otherwise stated. Then, the solvent was evaporated and the crude product was subjected to ^{1}H NMR analysis to determine the NMR yield and the d.r. value. Afterwards, the crude product of the reaction was dissolved in CH_2Cl_2 (0.25 M), and ethyl(triphenylphosphoranylidene)acetate (2.5 equiv.) was added. After stirring for 16 h, the crude mixture was directly purified by column chromatography on silica gel. The products were obtained as an inseparable mixture of *E* and *Z* isomers deriving from the Wittig derivatization. The enantiomeric excess was determined by ultra-performance convergence chromatography (UPC^2) analysis on the chiral stationary phase. For the preparation of the racemic products, see 'General procedure D' in Supplementary Information.

General procedure for the intermolecular preparation of enantioenriched cycloadducts

A 4-ml screw-cap vial equipped with a magnetic stirring bar was charged with the indole substrate (1 equiv.), the organocatalyst **2d** (20 mol%) and the appropriate olefin (3 equiv.) and filled with argon. Then, $CHCl_3$ (0.25 M) was added after being dried with 4-Å molecular sieves and degassed by sparging argon for 10 min. TFA was added (2.5 equiv.), and the vial was sealed. The mixture was irradiated for 18 h with a Kessil lamp set at 50% of its maximum output power, unless otherwise stated. Then, the solvent was evaporated and the crude product was subjected to ^{1}H NMR analysis to determine the NMR yield and the d.r. value. The crude mixture was directly purified by column chromatography on silica gel, affording the desired products. The enantiomeric excess was determined by UPC^2 analysis on chiral stationary phase. For the preparation of the racemic products, see 'General procedure F' in Supplementary Information.

Data availability

Details about materials, methods, experimental procedures, mechanistic studies, characterization data and NMR spectra are available in Supplementary Information. All calculations are provided electronically in the ioChem-BD Computational Chemistry repository at https://doi.org/10.19061/iochem-bd-6-426 (ref. 41). Crystallographic data for the structure reported in this article have been deposited at the Cambridge Crystallographic Data Centre under deposition no. CCDC 2392077 (**14**). Copies of the data are available via the Cambridge Crystallographic Data Centre at https://www.ccdc.cam.ac.uk/structures.

Acknowledgements

This work was supported by Ministero dell'Università PRIN 2020927WY3 (M.N. and L.D.), PRIN2022PNRR23_01 (L.D.) and European Research Council Starting Grant 2021 SYNPHOCAT 101040025 (L.D.). Chiesi Farmaceutici SpA and Dr Davide Balestri are acknowledged for support with the D8 Venture X-ray equipment. V.C. acknowledges financial support from the European Union's Horizon Europe research and innovation programme under Marie Skłodowska-Curie grant agreement PHOTO-STEREO no. 101106125. At the University of Pavia, S.A.S. thanks G. Colombo and the eos interdepartmental high performance computing facility for technical support and allocation of computational resources. S.A.S. also acknowledges D. Ravelli (University of Pavia) as well as P. García-Jambrina (University of Salamanca) and S. Gómez-Rodríguez (Autonomous University of Madrid) for very helpful discussions. Thanks are also due to I. Funes-Ardoiz (University of La Rioja) for assistance with the easyMECP.py code. We gratefully acknowledge the technical support units at the Department of Chemical Sciences of the University of Padova.

Author contributions

V.C. conceived of the project and devised the experiments with L.D. V.C., G.S. and L.R. carried out the reactions and isolated and characterized the products. V.C., G.S., L.R. and L.D. rationalized the experimental results. M.N. performed the spectroscopic investigations using transient absorption spectroscopy. S.A.S. performed the DFT and TD-DFT calculations. G.P. performed the X-ray analysis. V.C. and L.D. wrote the paper with contributions from all the authors. L.D. directed the work.

Competing interests

The authors declare no competing interests.

Additional information

Supplementary information The online version contains supplementary material available at https://doi.org/10.1038/s41557-025-01960-3.

Correspondence and requests for materials should be addressed to Luca Dell'Amico.

Peer review information *Nature Chemistry* thanks Martins Oderinde and the other, anonymous, reviewer(s) for their contribution to the peer review of this work.